Inorg. Chem. **2007**, *46*, 7341–7350

Ruthenium–Terpyridine Complexes with Multiple Ethynylpyrenyl or Ethynyltoluyl Subunits: X-ray Structure, Redox, and Spectroscopic Properties

Christine Goze,[†] Cristiana Sabatini,[‡] Andrea Barbieri,[‡] Francesco Barigelletti,*[,‡] and Raymond Ziessel*[,†]

Laboratoire de Chimie Moléculaire, École de Chimie, Polymères, Matériaux (ECPM), Université Louis Pasteur (ULP), 25 rue Becquerel, 67087 Strasbourg Cedex 02, France, and Istituto per la Sintesi Organica e la Fotoreattività, Consiglio Nazionale delle Ricerche (ISOF-CNR), Via P. Gobetti 101, 40129 Bologna, Italy

Received January 29, 2007

Several heteroleptic and homoleptic ruthenium–terpyridine complexes bearing two and four ethynylpyrenyl or ethynyltoluyl residues have been prepared from complexes carrying reactive bromo functions. Cross-coupling promoted by low-valent palladium(0) on these preformed complexes has advantageously been used to prepare the target complexes. The structure of a bis-terpyridine complex carrying four ethynylpyrenyl subunits was determined by single-crystal X-ray diffraction, showing a distorted octahedral geometry around the metal center, with the ethynylpyrenyl fragment being slightly tilted (about 5°) from the terpyridine plane. The molecular packing is characterized by intermolecular $\pi\cdots\pi$ interaction within dimers. The counteranions and the solvent molecules are entrapped in well-defined channels spanning along the *a*-axis. The complexes are redox active with a Ru oxidation overlapping the pyrene oxidation and two well-defined ligand-centered reduction processes. Pyrene reduction is irreversible and strongly cathodic. The new multichromophoric complexes are luminescent both in solution and in rigid matrix at 77 K, with room-temperature lifetimes and quantum yields significantly larger than those of $[Ru(terpy)_2]^{2+}$. At room temperature, the toluyl-substituted complexes are triplet metal-to-ligand charge-transfer (^{3}MLCT) emitters, whereas for the pyrene-grafted complexes pyrene-centered emission is observed. For the latter complexes, the energy gap, Δ_{TT}, between higher ^{3}MLCT levels and lower ligand-centered ($^3\pi\pi^*$, ^{3}LC) levels is in the 640–730 cm^{-1} range, which results in the interstate dynamics at the basis of the observed luminescent behavior. At 77 K, for the pyrene-grafted complexes, the emission reveals features that are tentatively ascribed to intraligand interactions involving the pyrene and terpyridine units.

Introduction

Ruthenium polypyridine complexes continue to play important roles in fields connected to solar energy conversion and the storage at the molecular level of light or electronic information or both.[1−5] The prototype of this class of compounds, $[Ru(bpy)_3]^{2+}$, has been one of the most studied metal-containing species in the last 2 decades (bpy = 2,2′-bipyridine).[6,7] Its homologous compound $[Ru(terpy)_2]^{2+}$, based on a tridentate polypyridine, is structurally more appealing than $[Ru(bpy)_3]^{2+}$ because of the absence of isomer problems (terpy = 2,2′: 6′,2″-terpyridine).[8] However, $[Ru(terpy)_2]^{2+}$ derivatives have much less attractive photophysical properties than $[Ru(bpy)_3]^{2+}$, most notably due to

* To whom correspondence should be addressed. E-mail: ziessel@chimie.u-strasbg.fr (R.Z.), franz@isof.cnr.it (F.B.).
[†] Université Louis Pasteur.
[‡] Istituto ISOF-CNR.

(1) Balzani, V.; Scandola, F. *Supramolecular Photochemistry*; Horwood: Chichester, U.K., 1991 (and references therein).
(2) Balzani, V.; Juris, A.; Venturi, M.; Campagna, S.; Serroni, S. *Chem. Rev.* **1996**, *96*, 759.
(3) Barigelletti, F.; Flamigni, L. *Chem. Soc. Rev.* **2000**, *29*, 1−12.
(4) Alstrum-Acevedo, J. H.; Brennaman, M. K.; Meyer, T. J. *Inorg. Chem.* **2005**, *44*, 6802−6827.
(5) Huynh, M. H. V.; Dattelbaum, D. M.; Meyer, T. J. *Coord. Chem. Rev.* **2005**, *249*, 457−483.
(6) Meyer, T. J. *Pure Appl. Chem.* **1986**, *58*, 1193−1206.
(7) Juris, A.; Balzani, V.; Barigelletti, F.; Campagna, S.; Belser, P.; Von Zelewsky, A. *Coord. Chem. Rev.* **1988**, *84*, 85.
(8) Sauvage, J.-P.; Collin, J.-P.; Chambron, J. C.; Guillerez, S.; Coudret, C.; Balzani, V.; Barigelletti, F.; De Cola, L.; Flamigni, L. *Chem. Rev.* **1994**, *94*, 993−1019.

10.1021/ic070149c CCC: $37.00 © 2007 American Chemical Society
Published on Web 08/04/2007

a short excited-state lifetime at room temperature.[9−11] Much efforts have been devoted to design tridentate ligands with prolonged lifetime,[12−14] including the use of cyclometalating ligands,[8] electron-withdrawing and electron-donor substituents,[15] and ligands with extended π^* orbitals.[12,16−19] Within the last approach, species based on ethynyl substitution have given quite interesting results.[19−21]

There has been recent interest in the study of bichromophores consisting of a Ru(II) tris-bidentate complex, $[Ru(N\wedge N)_3]^{2+}$, covalently linked to pyrene (and others)[22] using a variety of tethers.[22−31] For these compounds, the approach to generating long lifetime emission at room temperature is to select a ligand system whose lowest-lying ligand-centered ($^3\pi\pi^*$, ^{3}LC) level is slightly lower in energy relative to the metal-to-ligand charge-transfer (^{3}MLCT) emitting level of the complex core, with an energy gap of the order of k_BT, about 200 cm^{-1}. In such bichromophores at room temperature, visible light absorption results in a sequence of steps: (i) population of the ^{1}MLCT level at the $[Ru(N\wedge N)_3]^{2+}$ unit, (ii) rapid intersystem crossing to ^{3}MLCT and ^{3}LC states, (iii) establishment of thermal equilibrium between these two triplet levels, and (iv) light emission from the level with the higher radiative rate constant, k_r; for $[Ru(N\wedge N)_3]^{2+}$−pyrene systems this usually implies predominant emission from the ^{3}MLCT level (for the separate components, $\phi_{em}^{MLCT} > \phi_{em}^{LC}$, and $k_r^{MLCT} > k_r^{LC}$),[32] with the ^{3}LC level playing as "energy reservoir".[28,30,33−35] Of course, this scheme works well enough provided the two chromophores are only weakly interacting so that "localized" excitations can be considered. In most cases, the excited-state lifetimes observed from these complexes were significantly enhanced relative to model compounds as a result of the interstate dynamics involving ^{3}MLCT and ^{3}LC levels.[36,37]

It is interesting that also Ru(II) bis-terdentate complexes, $[Ru(N\wedge N\wedge N)_2]^{2+}$, have been covalently linked to pyrene in the attempt to enhance the ^{3}MLCT-based luminescence behavior.[21] Thus, in $[(pyr\text{-}terpy)Ru(terpy)]^{2+}$ the presence of the ethynyl-pyrene appendage results in an improved luminescence (by more than 2 orders of magnitude, for both the intensity and lifetime, $\phi = 5 \times 10^{-3}$ and $\tau = 580$ ns, respectively), with respect to the reference $[Ru(terpy)_2]^{2+}$ species (pyr-terpy = 4′(1-ethynyl-pyrene)-2,2′:6′,2″-terpyridine). Remarkably, the lowest-lying triplet in $[(pyr\text{-}terpy)Ru(terpy)]^{2+}$ was attributed of ^{3}MLCT nature.[21] Therefore, ^{3}LC (pyrene-centered) states, lying at higher energy, cannot apparently play as "energy reservoir" which leaves somewhat unexplained the reasons for the luminescence performance.

In the current work we present the synthesis, characterization, electrochemical behavior, and photophysical properties for a series of new Ru(II) complexes, Chart 1. Among these, **2a** and **3a** contain terpyridine ligands with ethynyl-pyrenyl substituents in the 5,5″ positions, and **2b** and **3b** can be regarded as appropriate model systems because they contain the ethynyl-toluyl subunits. The ethynyl-pyrenyl moiety appended to coordinating ligands has not only been employed in Ru(II)−polypyridine complexes, as mentioned above. Indeed, Pt(II)−bipyridyl and terpyridyl species incorporating the ethynyl-pyrenyl subunits are also known, and several of such complexes exhibit quite interesting luminescence properties.[38−41] Complexes **2a** and **3a** present room-temperature lifetimes larger by 2 orders of magnitude than those of $[Ru(terpy)_2]^{2+}$ with the emission mainly centered on the

(9) Lin, C. T.; Bottcher, W.; Chou, M.; Creutz, C.; Sutin, N. *J. Am. Chem. Soc.* **1976**, *98*, 6536−6544.
(10) Winkler, J. R.; Netzel, T. L.; Creutz, C.; Sutin, N. *J. Am. Chem. Soc.* **1987**, *109*, 2381−2392.
(11) Beley, M.; Collin, J. P.; Sauvage, J. P.; Sugihara, H.; Heisel, F.; Miehe, A. *J. Chem. Soc., Dalton Trans.* **1991**, 3157−3159.
(12) Medlycott, E. A.; Hanan, G. S. *Coord. Chem. Rev.* **2006**, *250*, 1763−1782.
(13) Wang, J. H.; Fang, Y. Q.; Bourget-Merie, L.; Poison, M. I. J.; Hanan, G. S.; Juris, A.; Loiseau, F.; Campagna, S. *Chem.−Eur. J.* **2006**, *12*, 8539−8548.
(14) Indelli, M. T.; Bignozzi, C. A.; Scandola, F.; Collin, J.-P. *Inorg. Chem.* **1998**, *37*, 6084−6089.
(15) Maestri, M.; Armaroli, N.; Balzani, V.; Constable, E. C.; Thompson, A. *Inorg. Chem.* **1995**, *34*, 2759−2767.
(16) Fang, Y. Q.; Taylor, N. J.; Hanan, G. S.; Loiseau, F.; Passalacqua, R.; Campagna, S.; Nierengarten, H.; Van Dorsselaer, A. *J. Am. Chem. Soc.* **2002**, *124*, 7912−7913.
(17) Passalacqua, R.; Loiseau, F.; Campagna, S.; Fang, Y. Q.; Hanan, G. S. *Angew. Chem., Int. Ed.* **2003**, *42*, 1608−1611.
(18) Duati, M.; Tasca, S.; Lynch, F. C.; Bohlen, H.; Vos, J. G.; Stagni, S.; Ward, M. D. *Inorg. Chem.* **2003**, *42*, 8377−8384.
(19) Encinas, S.; Flamigni, L.; Barigelletti, F.; Constable, E. C.; Housecroft, C. E.; Schofield, E. R.; Figgemeier, E.; Fenske, D.; Neuburger, M.; Vos, J. G.; Zehnder, M. *Chem.−Eur. J.* **2002**, *8*, 137−150.
(20) Harriman, A.; Ziessel, R. *Chem. Commun.* **1996**, 1707−1716.
(21) Hissler, M.; Harriman, A.; Khatyr, A.; Ziessel, R. *Chem.−Eur. J.* **1999**, *5*, 3366−3381.
(22) Wilson, G. J.; Launikonis, A.; Sasse, W. H. F.; Mau, A. W. H. *J. Phys. Chem. A* **1997**, *101*, 4860−4866.
(23) Ford, W. E.; Rodgers, M. A. J. *J. Phys. Chem.* **1992**, *96*, 2917−2920.
(24) Simon, J. A.; Curry, S. L.; Schmehl, R. H.; Schatz, T. R.; Piotrowiak, P.; Jin, X. Q.; Thummel, R. P. *J. Am. Chem. Soc.* **1997**, *119*, 11012−11022.
(25) Harriman, A.; Hissler, M.; Ziessel, R. *Phys. Chem. Chem. Phys.* **1999**, *1*, 4203−4211.
(26) Harriman, A.; Hissler, M.; Khatyr, A.; Ziessel, R. *Chem. Commun.* **1999**, 735−736.
(27) Tyson, D. S.; Bialecki, J.; Castellano, F. N. *Chem. Commun.* **2000**, 2355−2356.
(28) Tyson, D. S.; Henbest, K. B.; Bialecki, J.; Castellano, F. N. *J. Phys. Chem. A* **2001**, *105*, 8154−8161.
(29) Maubert, B.; McClenaghan, N. D.; Indelli, M. T.; Campagna, S. *J. Phys. Chem. A* **2003**, *107*, 447−455.
(30) Morales, A. F.; Accorsi, G.; Armaroli, N.; Barigelletti, F.; Pope, S. J. A.; Ward, M. D. *Inorg. Chem.* **2002**, *41*, 6711−6719.
(31) Schoonover, J. R.; Dattelbaum, D. M.; Malko, A.; Klimov, V. I.; Meyer, T. J.; Styers-Barnett, D. J.; Gannon, E. Z.; Granger, J. C.; Aldridge, W. S.; Papanikolas, J. M. *J. Phys. Chem. A* **2005**, *109*, 2472−2475.
(32) Montalti, M.; Credi, A.; Prodi, L.; Gandolfi, M. T. *Handbook of Photochemistry*, 3rd ed.; CRC Press, Taylor & Francis: Boca Raton, FL, 2006.
(33) Tyson, D. S.; Castellano, F. N. *J. Phys. Chem. A* **1999**, *103*, 10955−10960.
(34) Del Guerzo, A.; Leroy, S.; Fages, F.; Schmehl, R. H. *Inorg. Chem.* **2002**, *41*, 359−366.
(35) De Nicola, A.; Liu, Y.; Schanze, K. S.; Ziessel, R. *Chem. Commun.* **2003**, 288−289.
(36) McClenaghan, N. D.; Barigelletti, F.; Maubert, B.; Campagna, S. *Chem. Commun.* **2002**, 602−603.
(37) McClenaghan, N. D.; Leydet, Y.; Maubert, B.; Indelli, M. T.; Campagna, S. *Coord. Chem. Rev.* **2005**, *249*, 1336−1350.
(38) Michalec, J. F.; Bejune, S. A.; McMillin, D. R. *Inorg. Chem.* **2000**, *39*, 2708 ff.
(39) Michalec, J. F.; Bejune, S. A.; Cuttell, D. G.; Summerton, G. C.; Gertenbach, J. A.; Field, J. S.; Haines, R. J.; McMillin, D. R. *Inorg. Chem.* **2001**, *40*, 2193−2200.
(40) Pomestchenko, I. E.; Luman, C. R.; Hissler, M.; Ziessel, R.; Castellano, F. N. *Inorg. Chem.* **2003**, *42*, 1394−1396.
(41) Castellano, F. N.; Pomestchenko, I. E.; Shikhova, E.; Hua, F.; Muro, M. L.; Rajapakse, N. *Coord Chem. Rev.* **2006**, *250*, 1819−1828.

Chart 1. Structural Formulas[a]

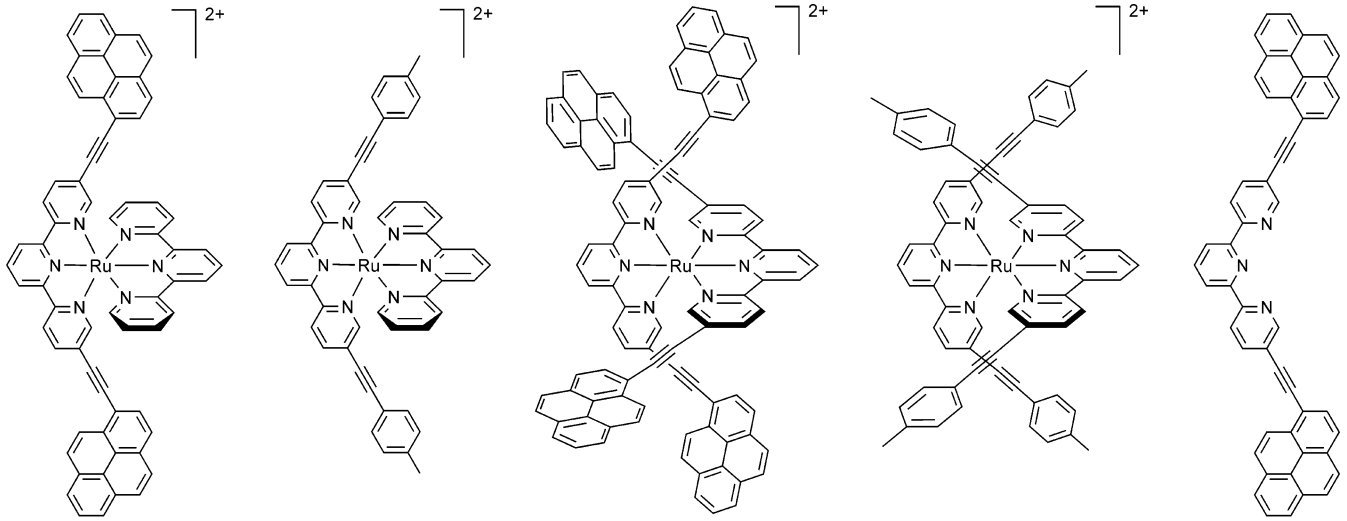

[a] **2** and **3** are the dibromo and tetrabromo precursor complexes, respectively; see the Experimental Section. All counteranions are hexafluorophosphates.

^{3}LC of the pyrene subunit, a behavior rarely reported.[42] For complexes **2a**, **2b**, **3a**, **3b** the luminescence results obtained at 77 K reveal a complicate interstate dynamics. In particular, a possible role of charge-transfer (CT) states of pyrene → terpy (or pyrene → ethynylterpy) nature is discussed.

Experimental Section

Structural formulas and abbreviations for the compounds studied are given in Chart 1.

General Methods. The ^{1}H and ^{13}C spectra were recorded at room temperature on Bruker AC 200 MHz, Bruker Avance 400 MHz, and Bruker Avance 300 MHz spectrometers at room temperature using perdeuterated solvents as internal standard: δ (H) in ppm relative to residual protiated solvent; δ (C) in ppm relative to the solvent. FT-IR spectra were recorded as KBr pellets. Fast atom bombardment (FAB, positive mode) mass spectra were recorded with ZAB-HF-VB-analytical apparatus with *m*-nitrobenzyl alcohol (*m*-NBA) as the matrix. Electrospray mass spectra (ES-MS) were recorded on a 1100 MSD Hewlett-Packard spectrometer.

Syntheses. 1-Bromopyrene, *p*-ethynyltoluene, trimethylsilylacetylene, NEt_3, and potassium hexafluorophosphate were obtained from commercial sources and used without further purification. 1-Ethynylpyrene, 5,5″-dipyrenyl-2,2′:6′,2″-terpyridine,[21] 5,5″-dibromo-2,2′:6′,2″-terpyridine,[43−45] Ru^{III}(2,2′:6′,2″-terpyridine)Cl_3,[46] and $[Pd(PPh_3)_4]$[47] were prepared and purified according to literature procedures. Diisopropylamine, acetonitrile, diethylether, and tetrahydrofuran were dried over suitable reagents and distilled under argon prior to use. CH_2Cl_2 and *i*Pr_2NH were distilled from P_2O_5 and KOH, respectively.

[Ruthenium(II)(5,5”-dibromo-2,2′:6′,2″-terpyridine)(2,2′:6′,2″-terpyridine)](PF$_6$)$_2$ (2). Ru(terpy)Cl_3 (0.07 g, 6.16 mmol) and $AgBF_4$ (0.095 g, 0.49 mmol) were refluxed for 2 h in acetone (35 mL). After cooling, the reaction mixture was filtered to remove AgCl, DMF (80 mL) was added, and the acetone was evaporated. The resulting solution was slowly added under argon to a hot solution (80 °C) of the ligand Br-terpy-Br (0.092 g, 0.24 mmol) in DMF (80 mL). The mixture was refluxed under argon during 1 h. DMF was then evaporated, acetonitrile (10 mL) was added, and the solution was treated with a saturated solution of potassium hexafluorophosphate in water. The precipitate was washed with water (20 mL) and ether (20 mL) and purified by column chromatography on silica ($CH_3CN/H_2O/KNO_3$, gradient 100:0:0 to 300:35:17). Recrystallization in CH_2Cl_2/hexane gave the desired compound (0.054 g, 33%). ^{1}H NMR (CD_3CN, 300 MHz): δ = 8.65 (dd, 4H, ^3J = 8.3 Hz, ^4J = 3.3 Hz), 8.50 (d, 2H, ^3J = 8.1 Hz), 8.48−8.39 (m, 2H), 8.38 (d, 2H, ^3J = 8.7 Hz), 8.10 (dd, 2H, ^3J = 8.7 Hz, ^4J = 2.1 Hz), 7.95 (td, 2H, ^3J = 8.1 Hz ^4J = 1.5 Hz), 7.36 (d, 2H, ^4J = 1.9 Hz), 7.31 (d, 2H, ^3J = 4.7 Hz), 7.29−7.16 (m, 2H). ^{13}C {^{1}H} NMR (CD_3CN, 75 MHz): δ = 159.1, 157.8, 156.4, 155.9, 154.0, 153.7, 141.9, 139.2, 137.4, 136.9, 128.4, 125.9, 125.7, 125.08, 125.1, 123.8. FT-IR (KBr, cm^{-1}): υ = 2923 (m), 1621 (m), 1438 (s), 1238 (m), 1114 (m), 875 (m), 832 (s), 762 (m), 554 (s). UV−vis (CH_3CN): λ nm (ϵ M^{-1} cm^{-1}): 475 (11 400), 320 (48 700), 282 (36 600), 270 (38 300). FAB$^+$ *m*/*z* (nature of peak): 869.1 ([M − PF_6]$^+$), 362.0 ([M − 2PF_6]$^{2+}$). Anal. Calcd for $C_{30}H_{20}Br_2F_{12}N_6P_2Ru$: C, 35.49; H, 1.99; N, 8.28. Found: C, 35.37; H, 1.74; N, 7.91.

[Ruthenium(II)(5,5″-dibromo-2,2′:6′,2″-terpyridine)$_2$](PF$_6$)$_2$ (3). Ru(Br-terpy-Br)Cl_3 (0.1 g, 0.17 mmol) and $AgBF_4$ (0.101 g, 0.52 mmol) were refluxed in air for 2 h in acetone (20 mL). After cooling, the reaction mixture was filtered under argon to remove AgCl, DMF (30 mL) was added, and the acetone was evaporated. The resulting solution was slowly added under argon to a hot solution (80 °C) of the ligand Br-terpy-Br (0.097 g, 0.25 mmol) in DMF (30 mL). After refluxing under argon for 3 h, DMF was evaporated, acetonitrile (10 mL) was added, and the solution was treated with a saturated solution of potassium hexafluorophosphate in water. The obtained precipitate was washed with water (30 mL) and ether (30 mL) and purified by column chromatography on alumina (CH_2Cl_2/MeOH, 100:0 to 90:10). Recrystallization in CH_2Cl_2/hexane gave the desired pure compound (0.14 g, 72%). ^{1}H

(42) Kozlov, D. V.; Tyson, D. S.; Goze, C.; Ziessel, R.; Castellano, F. N. *Inorg. Chem.* **2004**, *43*, 6083−6092.
(43) Colasson, B. X.; Dietrich-Buchecker, C.; Sauvage, J. P. *Synlett* **2002**, 271−272.
(44) Lehmann, U.; Henze, O.; Schluter, A. D. *Chem.—Eur. J.* **1999**, *5*, 854−859.
(45) Lehmann, U.; Schluter, A. D. *Eur. J. Org. Chem.* **2000**, 3483−3487.
(46) Sullivan, B. P.; Calvert, J. M.; Meyer, T. J. *Inorg. Chem.* **1980**, *19*, 1404−1407.
(47) Coulson, D. R. *Inorg. Synth.* **1972**, *13*, 121.

NMR (CD_3CN, 300 MHz): δ = 8.74 (d, 4H, ^3J = 8.1 Hz,), 8.42 (t, 2H, ^3J = 8.1 Hz), 8.36 (d, 4H, ^3J = 8.7 Hz), 8.10 (dd, 4H, ^3J = 8.7 Hz, ^4J = 2.1 Hz), 7.30 (d, 4H, ^4J = 2.1 Hz). ^{13}C {^1H} NMR (CD_3CN, 75 MHz): δ =158.1, 156.0, 154.4, 142.1, 137.5, 126.4, 125.5, 123.8. FT-IR (KBr, cm^{-1}): υ = 3449 (m), 1590 (m), 1443 (s), 1358 (m), 1231 (m), 1117 (m), 834 (s), 798 (m), 556 (s). UV−vis (CH_3CN): λ nm (ϵ M^{-1} cm^{-1}): 475 (11 200), 317 (66 200), 282 (47 800), 260 (43 100), 224 (43 900). FAB^+ *m*/*z* (nature of peak): 1029.1 ($[M - PF_6]^+$), 442.2 ($[M - 2PF_6]^{2+}$). Anal. Calcd for $C_{30}H_{18}Br_4F_{12}N_6P_2Ru$: C, 30.71; H, 1.55; N, 7.24. Found: C, 30.48; H, 1.65; N, 7.38.

General Procedure for the Preparation of the Ruthenium (II)−Pyrenes Complexes. In a Schlenk flask, to a stirred degassed acetonitrile/benzene (50:50) solution of the precursor complex, were added sequentially [$Pd(PPh_3)_4$], diisopropylamine, and the acetylenic ligand. The mixture was heated under argon for 16 h until the complete consumption of the starting material was observed. After the solution cooled to room temperature, potassium hexafluorophosphate in water was added and the solution was evaporated. The crude precipitate was washed two times with water and one time with diethyl ether and was purified by column chromatography. The fractions containing the pure complex were evaporated to dryness and recrystallized in CH_2Cl_2/hexane.

[Ruthenium(II)(5,5″-{1-ethynylpyrenyl}-2,2′:6′,2″-terpyridine)-(2,2′:6′,2″-terpyridine)](PF$_6$)$_2$ (2a). Prepared according to general conditions, from **2** (30 mg, 0.03 mmol) in acetonitrile (1.5 mL) and benzene (1.5 mL), 1-ethynylpyrene (17 mg, 2.5 equiv, 0.07 mmol), [$Pd(PPh_3)_4$] (2.1 mg, 6% mol), and *i*Pr_2NH (1 mL). The chromatography was performed on alumina (CH_2Cl_2/MeOH, 100:0 to 90:10), and recrystallization in CH_2Cl_2/hexane gave 20 mg of pure **2a** (53%). ^1H NMR (CD_3CN, 400 MHz): δ = 8.91 (d, 2H, ^3J = 8.5 Hz), 8.84 (d, 2H, ^3J = 8.5 Hz), 8.61−8.59 (m, 4H), 8.59 (t, 1H, ^3J = 8.0 Hz), 8.50 (t, 1H, ^3J = 8.0 Hz), 8.46 (d, 2H, ^3J = 9.0 Hz), 8.40 (d, 2H, ^3J = 7.5 Hz), 8.35 (d, 2H, ^3J = 7.5 Hz),8.29 (d, 2H, ^3J = 9.0 Hz), 8.26−8.22 (m, 6H), 8.18−8.12 (m, 6H), 8.00 (td, 2H, ^3J = 8.0 Hz, ^4J = 1.0 Hz), 7.65 (d, 2H, ^4J = 1.5 Hz), 7.47 (d, 2H, ^3J = 5.0 Hz), 7.27 (td, 2H, ^3J = 7.5 Hz, ^4J = 1.0 Hz). ^{13}C {^1H} NMR (CD_3CN, 100 MHz): δ = 159.2, 157.7, 156.5, 156.1, 152.5, 153.7, 140.8, 139.2, 137.2, 136.8, 133.3, 132.9, 132.1, 131.8, 130.8, 130.1, 130, 128.5, 128.1, 127.8, 127.3, 127.2, 125.8, 125.7, 125.6, 125.1, 125, 124.9, 124.8, 124.6, 116.3, 96.7 (C≡C), 90.4 (C≡C). FT-IR (KBr, cm^{-1}): υ = 3437 (m), 2925 (m), 2854 (m), 2193 (C≡C) (s), 1742 (s), 1620 (m), 1448 (s), 1261 (m), 1098 (m), 877 (m), 845 (s), 785 (m), 558 (s). UV−vis (CH_3CN): λ nm (ϵ M^{-1} cm^{-1}): 428 (38 300), 386 (32 200), 308 (45 000), 272 (42 400), 236 (57 100). FAB^+ *m*/*z* (nature of peak): 1161.2 ($[M - PF_6]^+$), 508.2 ($[M - 2PF_6]^{2+}$). Anal. Calcd for $C_{66}H_{38}F_{12}N_6P_2Ru{\cdot}CH_3CN$: C, 60.63; H, 3.07; N, 7.28. Found: C, 60.48; H, 2.97; N, 7.12.

[Ruthenium(II)(5,5″-bis{*p*-ethynyltoluyl}-2,2′:6′,2″-terpyridine)(2,2′:6′,2″-terpyridine)](PF$_6$)$_2$ (2b). Prepared according to the general conditions, from **2** (30 mg, 0.029 mmol) in acetonitrile (1.5 mL) and benzene (1.5 mL), *p*-tolylacetylene (18 μL, 5 equiv, 0.145 mmol), [$Pd(PPh_3)_4$] (2.1 mg, 6% mol), and *i*Pr_2NH (1 mL). The chromatography was performed on alumina (CH_2Cl_2/MeOH, gradient 100:0 to 90:10), and recrystallization in CH_2Cl_2/hexane gave 17.5 mg of pure **2b** (56%). ^1H NMR (CD_3CN, 300 MHz): δ = 8.80 (d, 2H, ^3J = 8.3 Hz), 8.75 (d, 2H, ^3J = 8.3 Hz), 8.55−8.40 (m, 6H), 7.99 (dd, 2H, ^3J = 8.3 Hz, ^4J = 1.9 Hz), 7.96 (td, 2H, ^3J = 7.9 Hz, ^4J = 1.3 Hz), 7.43 (d, 2H, ^4J = 1.3 Hz), 7.37−7.35 (m, 2H), 7.35 (d, 4H, ^3J = 8.1 Hz), 7.23 (d, 4H, ^3J = 8.1 Hz), 7.22−7.18 (m, 2H), 2.18 (s 6H). ^{13}C {^1H} NMR (CD_3CN, 75 MHz): δ = 159.1, 157.6, 156.4, 156.0, 155.0, 153.7, 141.6, 140.7, 139.2, 137.2, 136.8, 132.5, 130.5, 128.5, 125.6, 125.1, 125.05, 125.01, 124.9, 119.2, 97.8 (C≡C), 84.2 (C≡C), 21.4. FT-IR (KBr, cm^{-1}): υ = 3367 (m), 2919 (m), 2217 (C≡C) (m), 1594 (m), 1448 (s), 1244 (m), 1118 (m), 839 (s), 767 (m). UV−vis (CH_3CN): λ nm (ϵ M^{-1} cm^{-1}): 480 (9800), 334 (56 300), 308 (54 000), 270 (42 400), 236 (45 300). FAB^+ *m*/*z* (nature of peak): 941.2 ($[M - PF_6]^+$), 398.1 ($[M - 2PF_6]^{2+}$). Anal. Calcd for $C_{48}H_{34}F_{12}N_6P_2Ru$: C, 53.09; H, 3.16; N, 7.74. Found: C, 52.82; H, 2.91; N, 7.51.

[Ruthenium(II)(5,5″-bis{1-ethynylpyrenyl}-2,2′:6′,2″-terpyridine)$_2$](PF$_6$)$_2$ (3a). Prepared according the general conditions, from **3** (0.05 g, 0.04 mmol) in acetonitrile (2 mL) and benzene (2 mL), 1-ethynylpyrene (0.05 g, 5 equiv, 0.21 mmol), [$Pd(PPh_3)_4$] (0.017 g, 6% mol), and *i*Pr_2NH (1.5 mL). The chromatography was performed on alumina (CH_2Cl_2/MeOH, 100:0 to 90:10), and recrystallization in CH_2Cl_2/hexane afforded pure **3a** (0.045 g, 60%). ^1H NMR (CD_3CN, 400 MHz): δ = 9.31 (d, 4H, ^3J = 8.1 Hz), 9.01 (d, 4H, ^3J = 8.4 Hz), 8.86 (t, 2H, ^3J = 8.1 Hz), 8.48 (dd, 4H, ^3J = 8.4 Hz, ^4J = 1.8 Hz), 8.44−8.40 (m, 12H), 8.33 (d, 4H, ^3J = 9.2 Hz), 8.32 (d, 4H, ^3J = 8.8 Hz), 8.30 (d, 4H, ^3J = 8.1 Hz), 8.23 (d, 4H, ^3J = 9.1 Hz), 8.22 (d, 4H, ^4J = 2.1 Hz), 8.18 (t, 4H, ^4J = 7.6 Hz), 8.11 (d, 4H, ^3J = 8.1 Hz). ^{13}C {^1H} NMR (CD_3CN, 100 MHz): δ = 157.9, 156.1, 155.2, 140.7, 137.0, 132.9, 132.4, 131.7, 131.3, 130.2, 129.6, 127.6, 127.3, 127.0, 126.8, 125.24, 125.17, 125.0, 124.8, 124.6, 124.5, 124.2, 115.7, 106.5, 96.2 (C≡C), 90.1 (C≡C). FT-IR (KBr, cm^{-1}): υ = 3436 (m), 2922 (m), 21987 (C≡C) (s), 1588 (m), 1435 (s), 1117 (m), 840 (s), 714 (m), 557 (s). UV−vis (CH_3CN): λ nm (ϵ M^{-1} cm^{-1}): 427 (105 700), 388 (90 300), 360 (87 400), 324 (90 350), 280 (97 900), 236 (139 400). FAB^+ *m*/*z* (nature of peak): 1609.6 ($[M - PF_6]^+$), 732.3 ($[M - 2PF_6]^{2+}$). Anal. Calcd for $C_{102}H_{54}F_{12}N_6P_2Ru$: C, 69.82; H, 3.10; N, 4.79. Found: C, 69.56; H, 2.97; N, 4.45.

[Ruthenium(II)(5,5″-bis{*p*-ethynyltoluyl}-2,2′:6′,2″-terpyridine)$_2$](PF$_6$)$_2$ (3b). Prepared according the general conditions, from **3** (30 mg, 0.026 mmol) in acetonitrile (1.5 mL) and benzene (1.5 mL), *p*-tolylacetylene (32 μL, 10 equiv, 0.26 mmol), [$Pd(PPh_3)_4$] (2.1 mg, 6% mol), and *i*Pr_2NH (1 mL). The chromatography was performed on alumina (CH_2Cl_2/MeOH, gradient 100:0 to 97:3), and recrystallization in CH_2Cl_2/hexane afforded 21 mg of pure **3b** (62%). ^1H NMR (acetone-d_6, 300 MHz): δ = 9.09 (d, 4H, ^3J = 8.1 Hz), 8.81 (d, 4H, ^3J = 8.5 Hz), 8.62 (t, 2H, ^3J = 8.1 Hz), 8.14 (dd, 4H, ^3J = 8.5 Hz, ^4J = 1.9 Hz), 7.83 (d, 4H, ^4J = 1.5 Hz), 7.28 (d, 8H, ^3J = 8.1 Hz), 7.22 (d, 8H, ^3J = 8.1 Hz) 2.05 (s, 12H). ^{13}C{^1H} NMR (acetone-d_6, 75 MHz): δ = 157.2, 155.4, 154.4, 140.4, 140.2, 136.4, 131.5, 129.4, 124.5, 124.2, 124.0, 118.2, 96.7, ($CC_{ethynyl}$), 83.4, ($CC_{ethynyl}$), 20.6. FT-IR (KBr, cm^{-1}): υ = 3435 (m), 2919 (m), 2215 (C≡C) (s), 1590 (m), 1448 (s), 1243 (m), 1118 (m), 837 (s), 558 (m). UV−vis (CH_3CN): λ nm (ϵ M^{-1} cm^{-1}): 482 (11 600), 380 (86 900), 340 (110 500), 284 (67 800), 254 (57 400). FAB-*m*-NBA (CH_3CN): 1169.3 ($[M - PF_6]^+$), 512.3 ($[M - 2PF_6]^{2+}$). Anal. Calcd for $C_{66}H_{46}F_{12}N_6P_2Ru$: C, 60.32; H, 3.53; N, 6.40. Found: C, 60.11; H, 3.22; N, 6.21.

Electrochemical Measurements. Electrochemical studies employed cyclic voltammetry with a conventional three-electrode system using a BAS CV-50W voltammetric analyzer equipped with a Pt microdisk (2 mm^2) working electrode and a silver wire counter electrode. Ferrocene was used as an internal standard and was calibrated against a saturated calomel reference electrode (SCE) separated from the electrolysis cell by a glass frit presoaked with electrolyte solution. Solutions contained the electroactive substrate (≈1.5 mM) in deoxygenated and anhydrous dichloromethane or acetonitrile containing doubly recrystallized tetra-*n*-butylammonium hexafluorophosphate (0.1 M) as supporting electrolyte. The quoted half-wave potentials were reproducible within ≈15 mV.

Scheme 1[a]

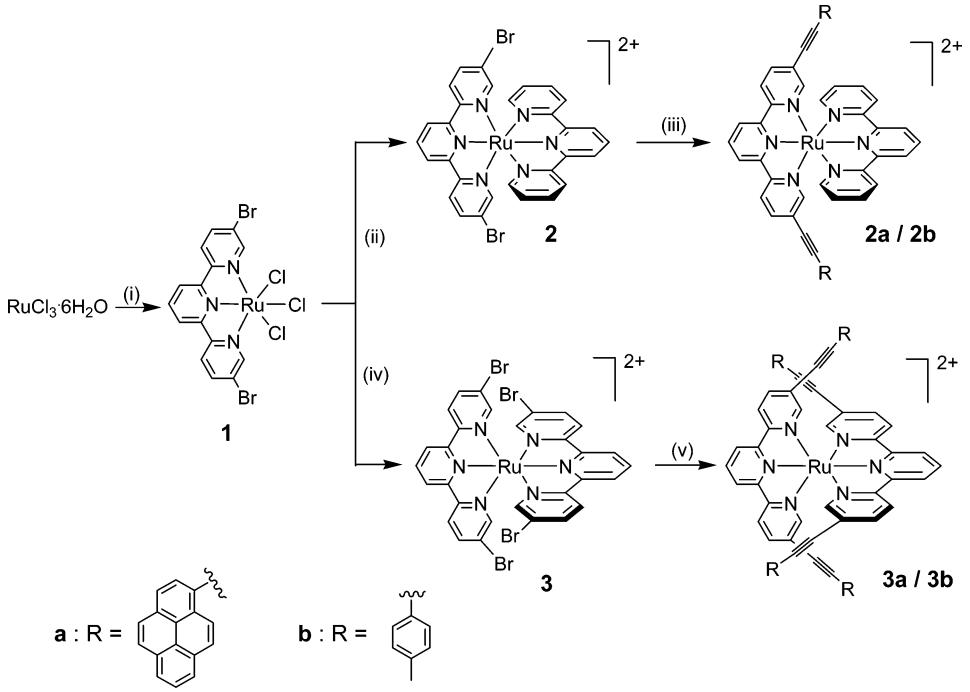

[a] (i) 5,5″-Dibromo-2,2′:6′,2″-terpyridine, EtOH, reflux, 3 h, 89%. (ii) (a) $AgBF_4$, acetone, reflux, 2 h; (b) terpy (1 equiv), DMF, reflux, 3 h; (c) KPF_6, 37%. (iii) (a) R-≡-H (2.5 equiv), [$Pd^0(PPh_3)_4$] 6 mol %, CH_3CN/C_6H_6 1:1, *i*Pr_2NH, 60 °C 16 h; (b) KPF_6, 52% for **2a** and 54% for **2b**. (iv) (a) $AgBF_4$, acetone, reflux, 2 h; (b) 5,5″-dibromo-2,2′:6′,2″-terpyridine (1 equiv), DMF, reflux, 3 h, 72%. (v) R-≡-H, [$Pd^0(PPh_3)_4$] 6 mol %, CH_3CN/C_6H_6 1/1, *i*Pr_2NH, 60 °C 16 h, 60% for **3a** and 62% for **3b**. All counteranions are hexafluorophosphates.

Optical Spectroscopy. UV−vis absorption spectra of dilute solutions (2×10^{-5} M) of CH_2Cl_2 (for the ligand) and CH_3CN (for the complexes) were obtained with Uvikon 933 or Perkin-Elmer Lambda 45 spectrometers. The luminescence spectra for O_2-free or air-equilibrated solutions at room temperature (absorbance <0.15 at the excitation wavelength) and at 77 K were measured by using a Spex Fluorolog II spectrofluorimeter with excitation wavelength λ_{exc} = 410 and 490 nm, for the ligand and the complexes, respectively. Corrected luminescence spectra were obtained by using a correction curve for the phototube response provided by the manufacturer. Luminescence quantum efficiencies (ϕ_{em}) were evaluated by comparing wavelength-integrated intensities (I) with reference to $[Ru(bpy)_3]Cl_2$ ($\phi_r = 0.028$, air-equilibrated water)[48] or quinine sulfate ($\phi_r = 0.546$, H_2SO_4 1 N)[49] and by using the following equation:[50]

$$\phi_{em} = \frac{A_r \eta^2 I}{\eta_r^2 I_r A} \phi_r \qquad (1)$$

where A and η are absorbance values (<0.15) at the employed excitation wavelength and refractive index of the solvent, respectively. Band maxima and relative luminescence intensities are obtained with uncertainty of 2 nm and 20%, respectively. The luminescence lifetimes of the complexes were obtained with an IBH 5000F single-photon equipment by using nanoled excitation sources at 373 (ligand) or 465 nm (complexes). Analysis of the luminescence decay profiles against time was accomplished by using software provided by the manufacturers. Estimated errors are 10% on lifetimes, 20% on quantum yields, and the working temperature was either 295 ± 2 K (1 cm square optical cells employed) or 77 K (with samples contained in capillary tubes immersed in liquid nitrogen).

Results and Discussion

Syntheses. Due to the pronounced insolubility of the pyrene-substituted terpyridine ligands, the target complexes were not synthesized according to classical procedures, consisting of binding the different ligands to the appropriate metal precursors. Similarly to their bipyridine analogues,[42,51,52] these molecules could be obtained from different starting materials containing unsubstituted terpyridine ligands and 5,5″-dibromo-2,2′:6′,2″-terpyridine ligands. Scheme 1 outlines the synthetic routes used for the generation of the metal complexes in this study. The pivotal bromo terpyridine complex **1** was prepared in a straightforward manner from $RuCl_3 \cdot 6H_2O$ and 5,5″-dibromo-2,2′:6′,2″-terpyridine. This complex was allowed to react with 2,2′:6′,2″-terpyridine or 5,5″-dibromo-2,2′:6′,2″-terpyridine to afford, respectively, complexes **2** and **3** in good yields. These precursor complexes could react smoothly under the Sonogashira−Hagihara conditions with 1-ethynylpyrene to provide the desired pyrenyl-substituted complexes **2a** and **3a** in fair yields. The current protocol is very interesting because it permits us, under mild conditions and in good yields, to introduce various ethynyl-grafted fragments. Moreover, the ethynyl-toluyl analogues **2b** and **3b** were synthesized, in order to have useful model compounds in view of the photophysical

(48) Nakamaru, K. *Bull. Chem. Soc. Jpn.* **1982**, *55*, 2967.
(49) Eaton, D. F. *Pure Appl. Chem.* **1988**, *60*, 1107−1114.
(50) Demas, J. N.; Crosby, G. A. *J. Phys. Chem.* **1971**, *7*, 991.
(51) Goze, C.; Kozlov, D. V.; Castellano, F. N.; Suffert, J.; Ziessel, R. *Tetrahedron Lett.* **2003**, *44*, 8713−8716.
(52) Goze, C.; Kozlov, D. V.; Tyson, D. S.; Ziessel, R.; Castellano, F. N. *New J. Chem.* **2003**, *27*, 1679−1683.

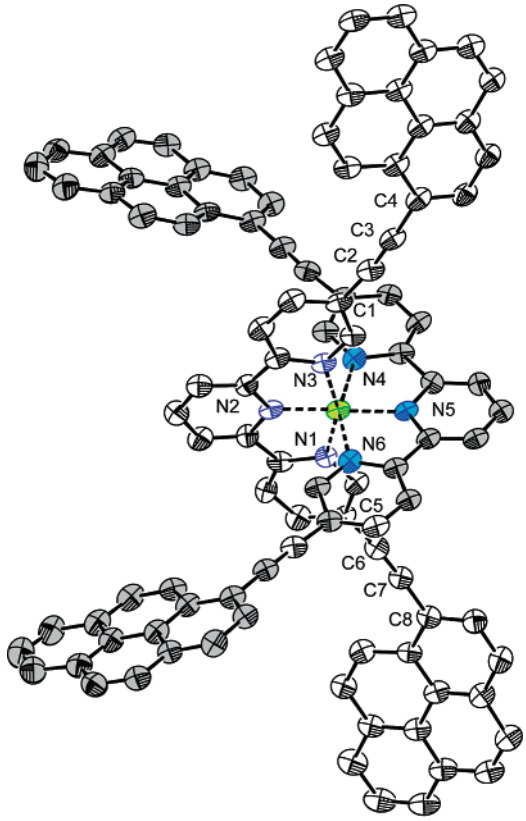

Figure 1. ORTEP view of complex **3a** with principal atomic numbering. Hydrogen atoms, solvent molecules, and counteranion are omitted for the sake of clarity. Thermal ellipsoids are at the 50% probability level.

investigations. The ligand 5,5″-diethynylpyrenyl-2,2′:6′,2″-terpyridine **4** was prepared independently to aid in spectroscopic assignments and appeared as expected very insoluble, thus limiting its complete characterization. All complexes were unambiguously characterized by NMR, FAB^+ or ESI spectroscopy, and FT-IR, and all data were consistent with the proposed structures.

X-ray Molecular Structure. Crystals of compound **3a** as the PF_6 salt were obtained by slow evaporation of a mixture of acetonitrile/toluene. The molecular structure, shown in Figure 1, exhibits a distorted octahedral geometry around the Ru center with the six nitrogen atoms provided by the two terpyridine ligands. The central $Ru-N_2$ (1.966 Å) and $Ru-N_5$ (1.967 Å) bond distances are similar to those found in $[Ru(terpy)_2](PF_6)_2$ (1.974 and 1.981 Å, respectively).[53] However, the Ru−N distances of the external pyridines (between 2.087 and 2.091 Å) are longer than those found in the reference compound (d_{Ru-N} = 2.065−2.076 Å) likely due to the pyrene residues involved in tight intermolecular packing. The bite angles N_6RuN_4 and N_1RuN_3 (157.43° and 157.42°) are similar to those of $[Ru(terpy)_2]^{2+}$ (158.4° and 159.1°). Crystallographic data are gathered in Table 1; selected bond distances and angles are listed in Table 2. Furthermore, the ethynylpyrenyl substituents are slightly tilted with respect to the terpyridine rings (4.9° and 5.6°). The crystal packing of the complexes revealed

(53) Lashgari, K.; Kritikos, M.; Norrestam, R.; Norrby, T. *Acta Crystallogr., Sect. C: Cryst. Struct. Commun.* **1999**, *55*, 64−67.

Table 1. Crystallographic Data for $[\mathbf{3a}](PF_6)_2 \cdot 3C_7H_8$

formula	$C_{102}H_{54}N_6Ru\ 2PF_6,\ 3C_7H_8$
M_r	2030.92
temp (K)	177 (2)
cryst syst	triclinic
space group	$P\bar{1}$
a [Å]	17.131(3)
b [Å]	18.134(3)
c [Å]	18.725(3)
α [deg]	108.97(5)
β [deg]	108.77(5)
γ [deg]	107.19(5)
V [Å^3]	4658(3)
λ [Å]	0.972
F(000)	2080
ρ_{calcd} [mg/m^3]	1.448
μ [mm^{-1}]	0.286
reflns collected/unique	27608/7693
θ range [deg] (completeness)	$2.62 < 2\theta < 27.65$
hkl range	$-0 \le h \le 16$; $-16 \le k \le 16$; $-17 \le l \le 16$
refined data/obs $I > 2\sigma(I)$	7693
restraints/params	3/755
goodness-of-fit on F^2	1.008
final R indices [$I > 2\sigma(I)$]	R1 = 0.087, wR2 = 0.233

Table 2. Selected Bond Distances (Å) and Angles (deg) for $[\mathbf{3a}](PF_6)_2 \cdot 3C_7H_8$

Ru−N1 2.087(28)	C1−C2 1.423(44)
Ru−N2 1.966(95)	C2−C3 1.195(38)
Ru−N3 2.091(26)	C3−C4 1.451(48)
Ru−N4 2.097(60)	C5−C6 1.430(57)
Ru−N5 1.967(93)	C6−C7 1.171(41)
Ru−N6 2.089(35)	C7−C8 1.470(48)
N3−Ru−N2 79.04(38)	C1−C2−C3 172.38(15)
N2−Ru−N1 78.38(38)	C2−C3−C4 177.14(15)
N3−Ru−N1 157.42(43)	C5−C6−C7 172.08(14)
N4−Ru−N5 78.75(41)	C6−C7−C8 176.80(14)
N5−Ru−N6 78.70(41)	
N4−Ru−N6 157.43(46)	

interesting features (Figure 2). A close look to the [100] projection revealed that the large channels are occupied by the PF_6 counteranions and residual toluene molecules (Figure 2a). The structural edifice is maintained by two types of pyrene−pyrene interactions forming dimers with $\pi\cdots\pi$ distances of 3.402 (Figure 2b) and 3.415 Å (Figure 2c). The dimers in Figure 2, parts b and c, weakly interact with neighboring dimers (average distance is 5 and 4 Å, Figure 2, parts b and c, respectively).

Electrochemical Behavior. Results from the cyclic voltammetric studies on the complexes in CH_3CN are collected in Table 3. For comparison purposes, literature data for 1-ethynylpyrenyl and $[Ru(terpy)_2]^{2+}$ are also included in Table 3.[8−11,21,25] The complexes containing bromo- and ethynyltoluyl-substituted terpy's, display a single and reversible oxidation step with an average separation between anodic and cathodic waves of 70 mV, that is largely independent of the scan rate in the range of 50−300 mV/s. This oxidation, occurring at +1.36, +1.43, +1.31, and +1.32 V for **2**, **3**, **2b**, and **3b**, respectively, is safely assigned to the Ru(III/II) couple as suggested by comparison with the reference complex $[Ru(terpy)_2]^{2+}$, +1.30 V;[11] all potentials are versus SCE. With respect to this unsubstituted complex, the bromo-substituted ones are more difficult to oxidize by 60 mV (case of **2**, with two Br centers) and 130 mV (case of **3**, four Br centers), reflecting the electron-withdrawing effect of the

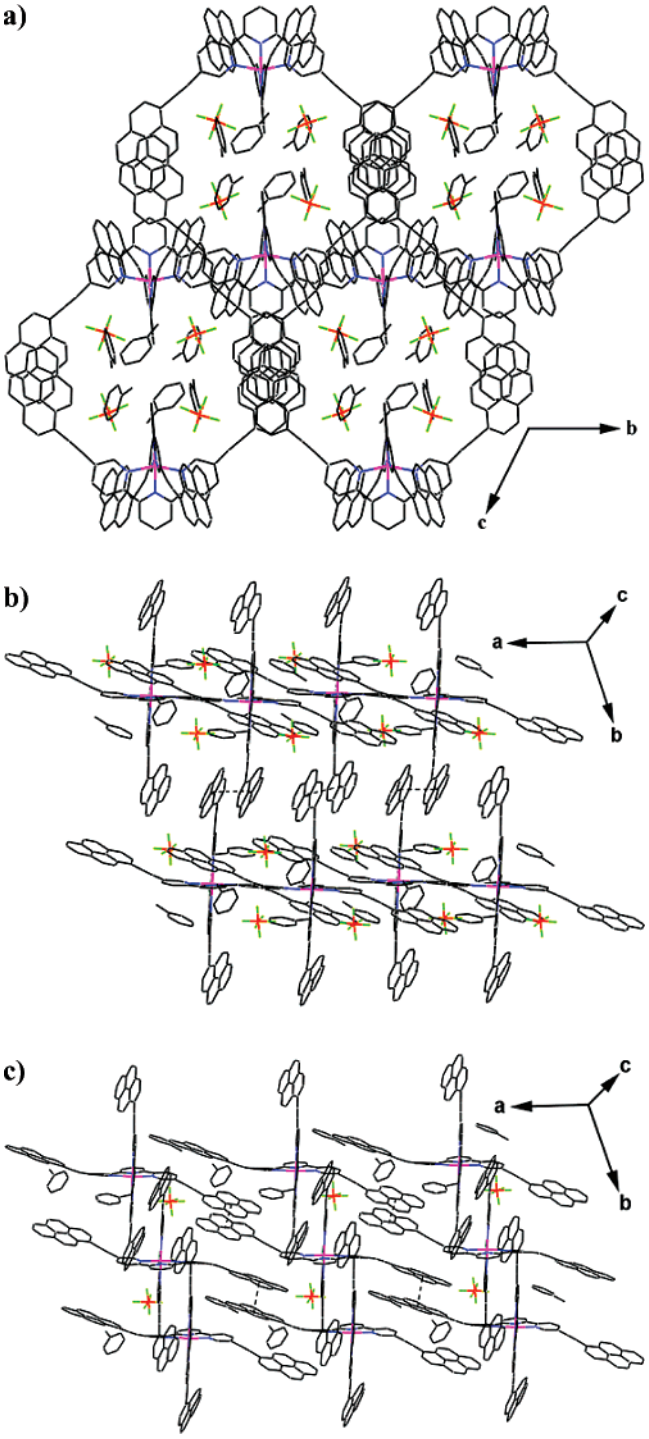

Figure 2. (a) Molecular packing of **3a** projected along the [100] direction. (b) Dimers at a distance of 3.402 Å (dashed lines). (c) Dimers at a distance of 3.415 Å (dashed lines).

halogen on the Ru oxidation process. By contrast, ethynyltoluyl substitution, cases **2b** (+1.31 V) and **3b** (+1.32 V), has little effect on the metal oxidation. When pyrene residues are grafted to the Ru complexes, cases of **2a** and **3a**, a broad irreversible oxidation wave is observed (Table 3), likely corresponding to an envelop of multiple redox processes. Actually, (i) the oxidation of ethynylpyrene (+1.47 V)[21,25] is expected to occur at a potential close to that of the Ru(II) center and (ii) the presence of multiple residues (two or four) reasonably accounts for multiple overlapping oxidation processes. Interestingly, only for **2a** at low temperature (230 K) a hump attributed to Ru(II) oxidation is observed at +1.40 V.

As expected, these complexes have several reversible ligand-based reductions, observed between −1.0 and −2.0 V with cathodic to anodic peak separation of 70 mV, independent of scan rates between 50 and 250 mV/s, Table 3. For the bromo complexes **2** and **3**, the first reduction is cathodically shifted by 190 and 230 mV and the second reduction is weakly shifted by 60 and 80 mV, respectively, with respect to what happens for $[Ru(terpy)_2]^{2+}$.[11] In contrast, for the ethynyl-toluyl complexes **2b** and **3b** the reduction potentials are anodically shifted by 110 and 70 mV, respectively, with respect to $[Ru(terpy)_2]^{2+}$ (Table 3). This shift reflects the better ability of the ethynyl-substituted terpy's to delocalize the excess charged embedded by the reduction. With regard to the complexes **2a** and **3a**, it is interesting to notice that, whereas free pyrene can be reduced at −2.09 V (vs SCE, DMF solvent)[32] and free 1-ethynylpyrene can be reduced at −1.78 V,[11] the +2 charge of the metal center is expected to further facilitate the reduction step for the bound pyrene fragment.[42] At any rate, for **2a** and **3a**, the first reduction is found easier than for the ethynyltoluyl-substituted complexes **2b** and **3b**, even if a more precise localization for the process, i.e., whether it occurs on the terpy or pyrene fragments, appears to be difficult. The second reduction wave, corresponding to a process involving the other coordinated ligand, approaches reversibility at scan rates greater that 100 mV/s where the anodic peak current starts to match that of the cathodic peak. Finally, the additional irreversible reduction around −1.75 V found for the pyrene-containing complexes, and absent in the others, is to be attributed to reduction of the terpyridine-pyrene fragment (or alternatively, to a pyrene-localized process if the first reduction was terpyridine-localized). This could result from a balance of effects traceable back to (i) the expected easier (first) reduction of bound ethynylpyrene with respect to what happens for free 1-ethynylpyrene[25] and (ii) the expected influence of the already reduced terpyridine-pyrene unit (or, according to a localized view, of the already reduced terpyridine fragment).

Steady-State Absorption and Luminescence Results. Ground-state absorption spectra are displayed in Figure 3, and concerned data for absorption and emission properties are collected in Table 4. Regarding the optical absorption properties, one can first notice that ligand **4** shows ethynylpyrenyl-based features in the region of 350−440 nm (absorption features for the terpy unit appear below 350 nm).[8−10] With regard to complexes **2b** and **3b**, the absorption features in the region of 320−400 nm can be ascribed to ^{1}LC transitions by the ethynyltoluyl groups (to notice the approximate doubling of molar absorptivity on passing from **2b** to **3b**, wherein two and four such units, respectively, are contained). For both complexes, the peak around 480 nm ($\epsilon_{480} \sim 11\,000$ M^{-1} cm^{-1}) is of ^{1}MLCT nature like for $[Ru(terpy)_2]^{2+}$, $\epsilon_{476} = 17\,700$ M^{-1} cm^{-1}.[8−11] The fact that for **2b** to **3b** the extinction coefficient in the region around 480 nm is lower than that for $[Ru(terpy)_2]^{2+}$ might suggest

Table 3. Electrochemical Data[a]

compd	$E^{0\prime}$(ox, soln) (ΔE) V (mV)	$E^{0\prime}$(red soln) (ΔE) V (mV)
2	+1.36 (70)	−1.43 (70), −1.57 (67)
2a	+1.59 (irrev, $I_a/I_c \approx 0.2$)(*)	−1.06 (70), −1.45 (80), −1.85 (irrev, $I_c/I_a \approx 0.1$)(*)
2b	+1.31 (70)	−1.13 (60), −1.47 (60)
3	+1.43 (70)	−1.47 (70), −1.59 (70)
3a	+1.69 (irrev, $I_a/I_c \approx 0.1$)(*)	−1.01 (60), −1.40 (60), −1.83 (irrev, $I_c/I_a \approx 0.1$)(*)
3b	+1.32 (70)	−1.17 (60), −1.50 (70)
1-ethynylpyrene[b]	+1.47 (70)	−1.78 (70)
$[Ru(terpy)_2]^{2+}$ [c]	+1.30 (60)	−1.24 (60), −1.51 (65)

[a] Potentials determined by cyclic voltammetry in deoxygenated CH_3CN solution, containing 0.1 M $TBAPF_6$, at a solute concentration of ca. 1.5 mM and at room temperature. Fc was used as an internal reference by assuming that $E_{1/2}(Fc/Fc^+) = +0.38$ V ($\Delta E_p = 60$ mV) vs SCE. Error in half-wave potentials is ±15 mV. For irreversible processes the peak potentials (E_{ap} or E_{cp}) are quoted. (*) Current ratios too far from unit are likely due to adsorption phenomena. All reversible redox steps result from a one-electron process. [b] References 21 and 25. [c] References 9−11.

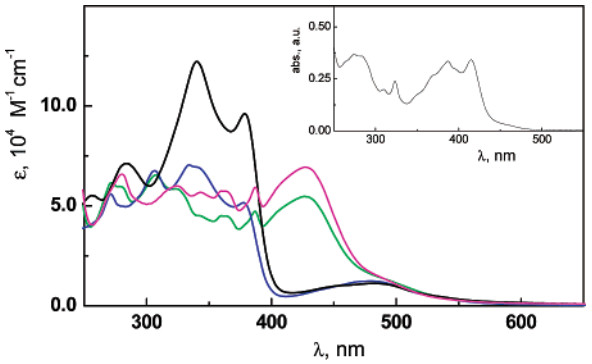

Figure 3. Absorption spectra of complexes **2a** (green), **3a** (magenta), **2b** (blue), and **3b** (black) in CH_3CN, and of ligand **4** (inset) in CH_2Cl_2.

subtle differences in the charge displacement mechanism for the CT transitions.[54−56] With regard to complexes **2a** and **3a**, the intense absorption ($\epsilon = 54\,400$ and $69\,800$ M^{-1} cm^{-1}, respectively) peaking at 428 nm can safely be ascribed to the involvement of pyrene units, as suggested by comparison with the absorption profile of ligand **4**, Figure 3. For this band, no doubling is observed in absorption intensity on passing from **2a** to **3a**; nevertheless, for the latter the absorption intensity is larger by ∼30% (Table 4), in line with the increased number of ethynylpyrenyl units. The nature of the band peaking at 428 nm can be ascertained by considering that ϵ_{428} is too high for a ^{1}MLCT transition, usually characterized by $\epsilon \leq 15\,000$ M^{-1} cm^{-1}.[6,7] For pyrene, the lowest-energy band system peaks around 400 nm with $\epsilon \sim 48\,000$ M^{-1} cm^{-1},[32] which, for both **2a** and **3a**, suggests a predominant ethynylpyrenyl -based ^{1}LC character for the band at 428 nm, that may include both $\pi\pi^*$ and intraligand charge-transfer (^{1}ILCT) contributions.[25,40]

A summary of the luminescence properties is reported in Table 4; Figures 4 and 5 display room-temperature and 77 K spectra, respectively; in all cases examined, the excitation spectra, as observed at the luminescence peak, overlapped with the absorption profiles. For the reference $[Ru(terpy)_2]^{2+}$ complex, it is well-known that the luminescence is very weak ($\lambda_{em} \sim 640$ nm, $\phi_{em} < 5 \times 10^{-5}$, $\tau < 1$ ns),[8−11] and this complex is regarded to be practically not luminescent. As it happens for all the members of the large family of Ru−polypyridine complexes, this is a consequence of the interplay of ^{3}MLCT states (responsible for the luminescence) and nonemissive ^{3}MC states.[7] The latter lie at higher energy and for cases wherein thermal equilibration establishes between them, the energy gap is frequently evaluated $\Delta > 2500$ cm^{-1}.[57] On the other hand, if the ^{3}MLCT and ^{3}MC levels are not thermally equilibrated, one must take into account a limiting kinetic case wherein the barrier between them, Δ', is apparently larger.[59] This is the case for $[Ru(bpy)_3]^{2+}$, $\Delta' \sim 4000$ cm^{-1},[7] and $[Ru(terpy)_2]^{2+}$, $\Delta' \sim 1600$ cm^{-1},[58] which results in the poor luminescence of the latter.

Given that $[Ru(terpy)_2]^{2+}$ offers a very convenient geometry for the development of multicomponent linear arrays, approaches have been developed to derivatize this basic unit, with the aim of enhancing its luminescence performances.[12,13,16−18,21] Within this perspective, and similar to what happens for $[Ru(bpy)_3]^{2+}$−pyrene derivatives,[12,22,23,28−30,36,60] it may be expected an interesting behavior for the pyrene-containing complexes examined here.[42] In fact, for several $[Ru(bpy)_3]^{2+}$−pyrene derivatives it happens that enhanced lifetimes can be observed based on the establishment of an equilibrium between individual ^{3}MLCT levels ($[Ru(bpy)_3]^{2+}$-centered) and ^{3}LC levels (pyrene-centered), provided these are sufficiently electronically decoupled.[30,36] To notice that, in these cases, λ_{em} and ϕ_{em} are notably found quite similar to those of the reference $[Ru(bpy)_3]^{2+}$ case.[12,22,23,28−30,36,60] This is explained by the very weak phosphorescence of pyrene; its lowest-lying ^{3}LC level features a low radiative rate constant ($\tau \sim 100$ μs, $1/\tau = (k_r + k_{nr})$, with $k_r < 10^3$ s^{-1}),[30,32] and this ^{3}LC level only plays the role of "energy reservoir" for the ^{3}MLCT emission of the metal-containing unit. For the understanding of this behavior, a key issue is the consideration of the energy gap, Δ_{TT}, between the lowest-lying ^{3}MLCT and ^{3}LC levels within the bichromophores. Provided the latter level lies only a few hundreds of wavenumbers below the ^{3}MLCT level,[30,36] an efficient

(54) Day, P.; Sanders, N. *J. Chem. Soc. A* **1967**, 1536.
(55) Phifer, C. C.; McMillin, D. R. *Inorg. Chem.* **1986**, *25*, 1329−1333.
(56) Damrauer, N. H.; Boussie, T. R.; Devenney, M.; McCusker, J. K. *J. Am. Chem. Soc.* **1997**, *119*, 8253−8268.
(57) Barigelletti, F.; De Cola, L.; Juris, A. *Gazz. Chim. Ital.* **1990**, *120*, 545−551.
(58) Hammarström, L.; Barigelletti, F.; Flamigni, L.; Indelli, M. T.; Armaroli, N.; Calogero, G.; Guardigli, M.; Sour, A.; Collin, J.-P.; Sauvage, J.-P. *J. Phys. Chem. A* **1997**, *101*, 9061−9069.
(59) Barigelletti, F.; Juris, A.; Balzani, V.; Belser, P.; Von Zelewsky, A. *J. Phys. Chem.* **1987**, *91*, 1095−1098.
(60) Wang, X. Y.; Del Guerzo, A.; Schmehl, R. H. *J. Photochem. Photobiol., C* **2004**, *5*, 55−77.

Table 4. Absorption and Emission Properties[a]

	absorption[b]	emission						
		295 K					77 K	
compd	λ_{max} (ϵ) nm (M^{-1} cm^{-1})	λ_{em} nm	ϕ_{em} 10^{-4}	τ ns	k_r[c] 10^4 s^{-1}	k_{nr}[c] 10^8 s^{-1}	λ_{em} nm	τ μs
2a	428 (54 400), sh480 (10 800)	672	4.0 (2.4)	89 (54)	0.45	0.112	724	6.7
2b	482 (10 800)	656	1.3 (1.3)	1.9 (1.9)	6.8	5.3	642	6.6
3a	428 (69 800), sh482 (10 600)	672	2.2 (1.4)	119 (75)	0.18	0.084	720	10
3b	480 (11 600)	640	0.7 (0.7)	0.54 (0.54)	13.0	18.5	636	6.2
4[d]	~416	487	700.0 (700.0)	2.3 (2.3)	3040	4.0	508	0.0095
$[Ru(terpy)_2]^{2+}$ [e]	476 (17 700)	~640	<0.5	<1			598	11

[a] In CH_3CN, unless otherwise indicated. The emission results are for O_2-free and air-equilibrated (within brackets) solvent; for the complexes, λ_{exc} was 490 nm for the spectra and 465 nm for the lifetimes; for ligand **4**, λ_{exc} was 420 nm for the spectra and 373 nm for the lifetimes. [b] Lowest-energy band. [c] From $k_r = \phi_{em}/\tau$ and $k_{nr} = 1/\tau - k_r$. [d] In CH_2Cl_2, too insoluble for absorption properties to be measured precisely. [e] References 8−11.

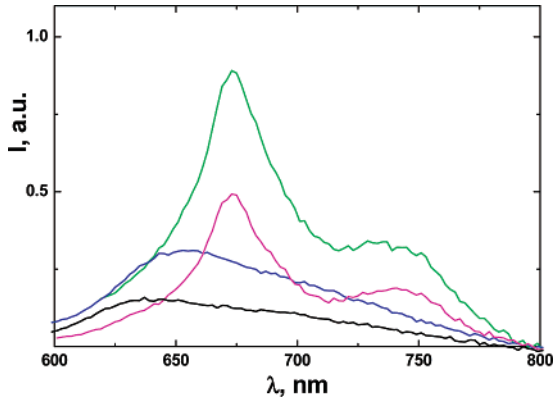

Figure 4. Room-temperature emission spectra of isoabsorbing CH_3CN solutions (λ_{exc} = 490 nm) of complexes **2a** (green), **3a** (magenta), **2b** (blue), and **3b** (black).

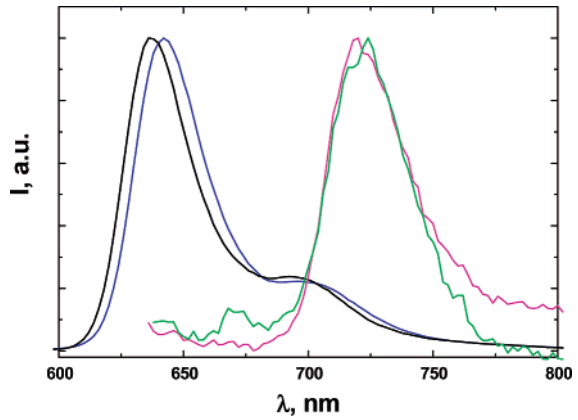

Figure 5. Normalized 77 K emission spectra of CH_3CN solutions of complexes **2a** (green), **3a** (magenta), **2b** (blue), and **3b** (black); λ_{exc} = 490 nm.

thermal redistribution between population of the upper (MLCT) and lower (LC) levels, N_{MLCT}/N_{LC}, can establish according to the Boltzmann equation, eq 2, with $k_BT = 205$ cm^{-1} at room temperature.

$$\frac{N_{MLCT}}{N_{LC}} = \exp\left(-\frac{\Delta_{TT}}{k_BT}\right) \qquad (2)$$

Regarding our present cases, the room-temperature luminescence profiles, lifetimes, quantum yields, and k_r values[61] (Figure 4 and Table 4) quite clearly indicate that **2b** and **3b** are ^{3}MLCT emitters, with properties, namely, $\phi_{em} = 7 \times 10^{-5}$ and $\tau = 0.54$ ns, very close to those of $[Ru(terpy)_2]^{2+}$. In contrast, the room-temperature luminescence features of **2a** and **3a**, are consistent with a ^{3}LC ($^3\pi\pi^*$) emission, as suggested by (i) the luminescence profiles (Figure 4), quite similar to previously reported pyrene-emitting cases,[28,30,40] and (ii) the k_r value (k_r in the range 10^3 s^{-1} in both cases, to be compared with $k_r \cong 8 \times 10^4$ s^{-1} for ^{3}RuLCT emitters[61] and $k_r < 10^3$ s^{-1} for pyrene[32]). Franck−Condon analysis of the luminescence profiles for **2a**, **3a**, **2b**, and **3b**, see the Supporting Information, provides approximate values for the energy gap, E_{00}, between the excited state associated with the emission and the ground state. For **2a** and **3a**, in order to draw estimates for the energy gap between the emissive ^{3}LC level and the higher-lying ^{3}MLCT levels, one can use the values for the ^{3}MLCT levels of **2b** and **3b** (that lack the pyrene units). Following this approach, the ^{3}LC−^{3}MLCT gap in **2a** and **3a** is estimated to be in the range of 640−730 cm^{-1} (see the Supporting Information). Therefore, upon thermal equilibration and according to eq 2, in both **2a** and **3a**, the fraction of molecules in their excited states with populated ^{3}LC levels, α, could be ca. 0.96 against a fraction of 0.04 with populated ^{3}MLCT levels, 1 − α.[30,33,36] On this basis, the enhanced luminescence properties of **2a** and **3a** at room temperature, with respect to the case of $[Ru(terpy)_2]^{2+}$, appear related to the stabilization of the emitting level (of ^{3}LC nature), resulting from thermal redistribution between ^{3}MLCT and ^{3}LC ($^3\pi\pi^*$) levels. Clearly, in this way, the higher-lying nonemissive Ru(II)-centered ^{3}MC states become thermally less accessible and less effective in depressing the overall luminescence output.[7]

It is interesting that in bichromophores of the type examined here, the luminescence quantum yield ϕ_{em} might be regarded to originate from a balance of two contributions, eq 3.[62]

$$\phi_{em} = \alpha\phi_{LC} + (1 - \alpha)\phi_{MLCT} \qquad (3)$$

This simple approach allows us to explain why in $[Ru(bpy)_3]^{2+}$−pyrene compounds, the emission is MLCT-centered at room temperature. In this case, $\phi_{MLCT} \sim 10^{-2}$,[7]

(61) Allen, G. H.; White, R. P.; Rillema, D. P.; Meyer, T. J. *J. Am. Chem. Soc.* **1984**, *106*, 2613−2620.

(62) Tsuboyama, A.; Iwawaki, H.; Furugori, M.; Mukaide, T.; Kamatani, J.; Igawa, S.; Moriyama, T.; Miura, S.; Takiguchi, T.; Okada, S.; Hoshino, M.; Ueno, K. *J. Am. Chem. Soc.* **2003**, *125*, 12971−12979.

ϕ_{LC} is lower by orders of magnitude,[32] and $(1 - \alpha)\phi_{MLCT} \gg \alpha\phi_{LC}$, eq 3. In contrast, for $[Ru(terpy)_2]^{2+}$−pyrene bichromophores at room temperature, $\phi_{MLCT} < 10^{-4}$, apparently resulting in $(1 - \alpha)\phi_{MLCT} \ll \alpha\phi_{LC}$. As a consequence, the emission is expected to be pyrene-centered, like it actually happens in **2a** and **3a** and the other few cases reported previously.[42]

Regarding emission data for **2a** and **3a** at 77 K, predictions based on eqs 2 and 3 are somewhat conflicting. This is because (i) the thermal redistribution (see eq 2) is expected to favor population by a factor $\sim 10^4$ of the lower-lying ^{3}LC level against the ^{3}MLCT level, however (ii) the luminescence quantum yield for a $[Ru(terpy)_2]^{2+}$-type emitter undergoes a relevant increase, with $\phi_{MLCT} \cong 0.5$ at 77 K,[8] again, by a factor $\sim 10^4$. On these bases, it seems that the two opposite effects are likely to counterbalance each other. The luminescence results at 77 K, Table 2 and Figure 5, are indeed controversial also because ILCT levels (that we tentatively indicate as pyrene-to-terpy or pyrene-to-ethynylterpy, for **2a** and **3a**) might be involved, as discussed below.

Upon going from room temperature to 77 K, MLCT emitters are expected to exhibit a blue-shift in a polar solvent.[7] This is due to the fact that in frozen solvent, the solvent molecules cannot respond to the changes in molecular polarity (consequent to CT transitions), and one observes the emission from a destabilized level with respect to the fluid (room-temperature) case. Consistent with this, for **2b** and **3b** (CT emitters at room temperature), the peak of the 77 K emission undergoes a slight hypsochromic shift with respect to ambient temperature (Table 4).

In contrast, for **2a** and **3a** and on passing from room temperature to 77 K a pronounced red-shift of the emission peak is registered (with $\lambda_{max} \sim 724$ and 720 nm, respectively, Table 4), a behavior suggesting an LC emission. However, although at room temperature the luminescence profiles for both **2a** and **3a** are consistent with a ^{3}LC ($\pi\pi^*$) pyrene-based emission (Figure 4), their 77 K luminescence profiles, Figure 5, are broad like it happens for CT states and are not at all reminiscent of a pyrene-like character,[42] like that found at room temperature (see above). This observation is corroborated by the detected lifetimes, 6.7 and 10 μs for **2a** and **3a**, respectively, again typical for ^{3}CT emitters at this temperature.[7,8] Thus, for **2a** and **3a** at 77 K, the luminescence results do not support an assignment to ^{3}LC ($^3\pi\pi^*$, pyrene-like) levels.

It is interesting that for the room-temperature LC emission from Pt(terpy-pyrene)Cl^+ a partial ^{3}ILCT character (pyrene → terpy) was established.[38,39] In that case (i) the lowest-lying triplet level was found to peak at 700 nm, (ii) the next higher-lying level was separated by an energy gap of some 1000 cm^{-1}, and (iii) in the presence of oxygen, only the latter was found to be luminescent, an outcome explained by a substantial singlet character,^{1}(ILCT/MLCT), of the higher-lying state. These findings suggest that low-lying CT states (possibly, ILCT states at the ethynyl-pyrenyl subunits), could play a role also for **2a** and **3a**.[25,34,38,40] Indeed, for these complexes the detected emission (phosphorescence) at 77 K peaks in the same energy region ($\lambda_{em} = 724$ and 720 nm, respectively) of the room-temperature ^{3}ILCT (pyrene → terpy) emission from Pt(terpy-pyrenel)Cl^+, $\lambda_{em} = 700$ nm.[38] The fact that for **2a** and **3a** at 77 K one observes a low-lying phosphorescence of ^{3}CT nature that goes undetected at room temperature (where the emission comes instead from ^{3}LC pyrene levels, higher in energy by some 1000 cm^{-1}) is an unusual occurrence. It may be that rigidification of the solvent at 77 K causes changes in the structural arrangement of the spatially extended pyrene-containing fragments and enhances intercomponent interactions that go undetected in room-temperature fluid solvent.

In conclusion, at room temperature, both **2a** and **3a** exhibit a pyrene-centered emission. In these complexes, and taking **2b** and **3b** as reference cases (Table 4, and Figure 4), the energy gap between ^{3}MLCT and ^{3}LC levels is large enough (Δ_{TT} in the range of 600−700 cm^{-1}, eq 2), to lead to predominant population of the lower ^{3}LC level. For both **2a** and **3a** the room-temperature lifetimes are well larger (and likewise the luminescence quantum yields) than for the case of $[Ru(terpy)_2]^{2+}$, Table 4. This outcome is of interest within the perspective of looking for Ru−terpy-type derivatives with improved luminescence features.[12,13,16−18,60]

Acknowledgment. The authors thank CNRS and IST/ILO Contract 2001-33057 for funding. We are also indebted to Dr. Franck Camerel (ECPM/LCM Strasbourg) and Dr. Pascal Retailleau from the Service de Cristallochimie at the ICSN-CNRS in Gif-sur-Yvette (Paris), for carefully checking the crystals data and analyzing the molecular packing. Thanks are also due to Project MACOL PM.P04.010 of CNR, Italy.

Supporting Information Available: Crystallographic data and energy gap data. This material is available free of charge via the Internet at http://pubs.acs.org.

IC070149C